

Triple Analysis of the Cancer Epigenome: An Integrated Microarray System for Assessing Gene Expression, DNA Methylation, and Histone Acetylation¹

Huidong Shi, Susan H. Wei, Yu-Wei Leu, Farahnaz Rahmatpanah, Joseph C. Liu, Pearly S. Yan, Kenneth P. Nephew, and Tim Hui-Ming Huang^{2,3}

Department of Pathology and Anatomical Sciences, Ellis Fischel Cancer Center, University of Missouri School of Medicine, Columbia, Missouri 65203 [H. S., S. H. W., Y-W. L., F. R., J. C. L., P. S. Y., T. H-M. H.]; Medical Sciences, Indiana University School of Medicine, Bloomington, Indiana 47405 [K. P. N.]; and Departments of Cellular and Integrative Physiology, and Obstetrics and Gynecology, Indiana University Cancer Center, Indianapolis, Indiana, 46202 [K. P. N.]

ABSTRACT

We developed a novel microarray system to assess gene expression, DNA methylation, and histone acetylation in parallel, and to dissect the complex hierarchy of epigenetic changes in cancer. An integrated microarray panel consisting of 1507 short CpG island tags located at the 5'-end regions (including the first exons) was used to assess effects of epigenetic treatments on a human epithelial ovarian cancer cell line. Treatment with methylation (5-aza-2'-deoxycytidine) or deacetylation (trichostatin A) inhibitors alone resulted in up-regulation of 1.9 or 1.1% of the genes analyzed; however, the combined treatment resulted in synergistic reactivation of more genes (10.4%; $P < 0.001$ versus either treatment alone). On the basis of either primary or secondary responses to the treatments, genes were identified as methylation-dependent or -independent. Synergistic reactivation of the methylation-dependent genes by 5-aza-2'-deoxycytidine plus trichostatin A revealed a functional interaction between methylated promoters and deacetylated histones. Increased expression of some methylation-independent genes was associated with enhanced histone acetylation, but up-regulation of most of the genes identified using this technology was because of events downstream of the epigenetic cascade. We demonstrate proof of principle for using the triple microarray system in analyzing the dynamic relationship between transcription factors and promoter targets in cancer genomes.

INTRODUCTION

Microarray approaches used to study functional DNA-protein interactions (1–3) have revealed recently that many transcription regulators are linked to chromatin remodeling (3, 4), placing this type of epigenetic change at the center of gene regulation. Repressed chromatin and gene silencing are associated with changes in DNA methylation and histone acetylation (5), and whereas these epigenomic modifications are widely recognized as contributing factors in human tumorigenesis, their molecular basis is not understood yet. One model suggests that methylated DNAs at the 5'-end regulatory regions recruit MBD⁴ proteins, which are known to complex with HDACs and other transcriptional corepressors (6). Deacetylation of lysine groups on histones 3 and 4 occurs via HDACs, resulting in a tighter interaction between negatively charged DNA and positively charged lysine, and a closed, repressive chromatin configuration (5, 6). How repressive chromatin structures assemble onto DNA is not clear, but changes

in methylation status of CpG islands in gene promoters presumably play a central role (5). We developed recently a microarray approach called differential methylation hybridization for screening CpG methylation and identifying loci susceptible to epigenetic modifications in various cancers (7–9). However, to fully elucidate the functional relationship between DNA methylation and histone acetylation in gene silencing, a genomic microarray system for detecting changes in gene expression, DNA methylation, and histone acetylation would be necessary.

We developed an integrated “triple” microarray system to decipher the hierarchies of epigenetic regulation of gene expression in cancer cells. The microarray panel used in this novel approach contains 1507 ECISTs, short genomic fragments (0.2–2-kb) located at the 5'-end regulatory regions of genes (10). We used the GC-rich components of ECISTs for screening methylated CpG sites, the exon-containing portions (*i.e.*, the first exons) for measuring levels of the corresponding transcripts, and the promoter sequences within ECISTs for identifying chromatin immunoprecipitated with antibodies against acetylated histones. It is well known that DNA methylation and histone acetylation work in concert to regulate gene expression, and this new microarray system provides an effective means of segregating at specific loci expression changes that occurred as a consequence of reversing promoter hypermethylation status by epigenetic treatments.

MATERIALS AND METHODS

Cell Culture. A human epithelial ovarian cancer cell line CP70 (gift from Dr. Robert Brown, University of Glasgow, Glasgow, United Kingdom) was cultured in the presence of vehicle (PBS) or DAC (0.5 μ M; medium changed every 24 h). After 4 days, cells were either harvested or treated with TSA (0.5 μ M) for 12 h and then harvested. Some cells were also treated with TSA alone for 12 h before harvest. DNA and RNA were isolated using the QIAamp Tissue and RNeasy kits (Qiagen), respectively.

Microarray Screening of ECISTs. To identify ECISTs (including the first exons), RLCS (11) was used to prepare targets for screening of CpG island clones derived from a genomic library, CpG Island library (12). In the presence of T4 RNA ligase, an RNA adapter (0.5 nmol, 5'-ACC GGA GCG GCA CGG GAA AUA GAG CAA CAG GAA A) was ligated to the 5'-ends of decapped mRNAs derived from the Stratagene Human Universal Reference RNAs. After reverse transcription, full-length cDNAs were amplified by long RT-PCR (TaqPlus Long PCR system; Stratagene) with the flanking 5'- and 3'-adapters (5'-GCA CGG GAA ATA GAG CAA CAG and 5'-GGC CGA CTC ACT GCG CGT CTT CTG, respectively). A low number of PCR cycles (18–25) were used to preserve the linearity of amplification. Amplified products were labeled with Cy3 fluorescent dyes as described (10) and hybridized to the CGI microarray panel. Hybridization and posthybridization procedures were performed.⁵ Hybridized slides were scanned with the GenePix 4000A (Axon). The acquired images and data were transferred to Excel spreadsheets for additional analysis using GenePix Pro 3.0. CGI loci with signal intensities 2-fold greater than local background were scored as positive for containing expressed sequences.

Methylation Microarray Analysis. Preparation of methylation amplicons was carried out essentially as described (7). Briefly, CP70 DNA (~1 μ g) was

Received 12/3/02; accepted 2/28/03.

The costs of publication of this article were defrayed in part by the payment of page charges. This article must therefore be hereby marked *advertisement* in accordance with 18 U.S.C. Section 1734 solely to indicate this fact.

¹ Supported in part by National Cancer Institute Grants CA-85289 (to K. P. N.), -69065, and -84701 (to T. H-M. H.), and by Epigenomics, Inc. T. H-M. H. was a recipient of a travel fellowship from the Foundation for Promotion of Cancer Research, Japan.

² To whom requests for reprints should be addressed, at Department of Pathology and Anatomical Sciences, Ellis Fischel Cancer Center, University of Missouri, 115 Business Loop I-70 West, Columbia, MO 65203. Phone: (573) 882-1276; Fax: (573) 884-5206; E-mail: huangh@health.missouri.edu.

³ T. H-M. H. is a consultant to Epigenomics, Inc.

⁴ The abbreviations used are: MBD, methyl-CpG binding domain; HDAC, histone deacetylase; ECIST, expressed CpG island sequence tag; DAC, 5-aza-2'-deoxycytidine; TSA, trichostatin A; RLCS, RNA ligase-mediated cDNA synthesis; ChIP, chromatin immunoprecipitation; COBRA, combined bisulfite restriction analysis; RT-PCR, reverse transcription-PCR.

⁵ Internet address: <http://www.microarrays.org>.

Table 1 Primer sequences used for triple analysis^a

Clone ID	Gene	Strand	COBRA primers (5'→)	ChIP-PCR primers (5'→)	RT PCR primers (5'→)
SC21G11	<i>HSPA.2</i>	Forward	TGTTGATGATGGGGTTGTAAT	TTCGATGGTGGTCCCCGGAG	GCACCGGTAAGGAAAACAAA
		Reverse	ACAAAATCACCATCACCAATAAC	GGGCAAGATTAGCGAGCAGGA	GAGCCAGTTGATCACCTCTG
CpG5B6	<i>CYP27B1</i>	Forward	AGGGGTTGAGATATGATGTTTAGG	TCTGGCCGAACCTTTCTGCAA	TCTGCTTCTGGCCCTTCTG
		Reverse	ACCATTTTCCCCAACACTCTATC	CCTCAACTCGCTTTTCCTTA	TCCCTTCTGCCACATGGTTCA
SC87F10	<i>EIF1A</i>	Forward	TTTATTTTTATTTTTGGGTATGG	TGCGCCATTTCCCAACATTTTG	ATGCTAAAATCAATGAACTG
		Reverse	CCATAAAACCACCCACCACA	TGTCGCCCTCAGAGCAGCAG	TCTTCTACCCATAAGCTCCAT
SC10H6	<i>KIAA0560</i>	Forward	GTATAGAGGAGGTTAAAGTTTTTGG	TGGGCTGTTGTACGGGTTCC	CCTGCATGAACCTCCGGCTAC
		Reverse	CCATAACAACACTCTTCCCTCC	GGTCACGAACCTCCGCATTGAT	GGTCACGAACCTCCGCATTGAT
DL3D6	<i>FLJ31663</i>	Forward	TTTTATTAATGGTGGTGTAGAA	TCTTCTCCATTCGCTGTC	CCTGGCAGCCTAACCCCTC
		Reverse	CCAACCTTCTCTTCTCTTCTC	CCTTTACACTTCCGGTTCACT	CACCTTCTAGTGTCCGGTTGA
SC28C11	<i>TAF2K</i>	Forward	GGTTGGTTTTTGTAGTTGGTTATATTA	CCCCGAACCTGTCCGCTGAATTCAC	TGGAGGAGGTGCAGAAGGTGG
		Reverse	CTACTAACTTACCCTCTATAATCC	AGCCGGCAGACGCTGTGAGT	TCCTTGGGTCTTTCGAATCA
SC12E1	<i>IER-3</i>	Forward	GTGATTTTTYGTATTTTTAAGAAGAA	CTGGCGACCGAAGCAGACTGC	GCCCTAACGCCGACTCCCTG
		Reverse	AACCTAACCCCAACTAAACTATACC	TTGGCGGGTCTCTTAACCT	TCTGTGCGCCTCGTCCCGC
SC13E11	<i>TIGA1</i>	Forward	TTTGGTTTTTTGGGATG	CAGGCCTGGAGCATAGTAAG	GCATTGTGGGACGGAAGC
		Reverse	TATCTAAAAAATCCCTAACATAATC	CAGTGAGGGACCGAGGG	AACCTCCCTGGCATAGTCCGATG
SC13C2	Predicted	Forward	GATTTTTGTAAATTAGTTTGTATGTGT	GCCTGATCCACGCCGATTG	GTTCGAGGTCGTCATGGCTG
		Reverse	AATTTCCACTCYCCTATCATAACATC	GGCTGCCGAGAAGGTAGGAG	TTTCATCTGGTGGCCCTAGCG
SC10B6	<i>MDS1</i>	Forward	ATTTTTTTGGTGTGTTTGTATG	ACAAGCTTGTGGCGATTCTA	ATCCAGACCTTGAAGTCCGCT
		Reverse	CCTACCATAAAAATAAAATCACCA	AGTTTGGACACCTTCGCAC	CAAGTAATCTGGGGAACCGAT
SC69A9	<i>UNG2</i>	Forward	TTGTAAGTTGTTTAGTTGGTTGAT	TCCAGTTCCATTGCGTTTCT	TCCAGTTTCCATTGCGTTTCT
		Reverse	ATAAATTTCTAAAAACCCAACTA	CAGGCACAGCGACTCGAA	CAGGCACAGCGACTCGAA
Control	<i>GTF2H4</i>	Forward	TCAAATCTCCAGGAGCCAATG	TTTGTAGTCAGACGCGCTTCA	ATTAAGCGACGCGCCGAGAC
		Reverse	CTATCTCTTAACCCACTTCTACTA	CATTGGCTCCTGGAGATTGA	CCAGAAAGAGCATCCGCATCA
Control	<i>FLJ31996</i>	Forward	GTATTGAGTAGTTTTATTAYGGAGT	CTCAGGCCGCTTAGTCAAAT	TTGCGGCTCCGTTGGT
		Reverse	AAAACAACATATCACTAAACCCT	GGAGCCGCAAGTAACGACA	GGTTTCGGCCAGTGTGACAT
Control	<i>β-Actin</i>	Forward	—	—	GGATTCTATGTGGGCGACGAG
		Reverse	—	—	CGCAGCTCATTGTAGAAGGTGTGG

^a R, mixture of A and G; Y, mixture of G and T.

digested with *MseI* and then ligated to a PCR-linker. The ligated DNA was digested with methylation-sensitive endonucleases *BstUI* and *HpaII*, and amplified with a linker primer by PCR. DNA obtained from a normal ovary tissue was prepared similarly. Genomic fragments containing methylated sites were protected from enzymatic restrictions and could be amplified; however, fragments containing unmethylated sites were digested and, thus, not present in the amplified samples. CP70 amplicon was labeled with Cy5 (red), whereas the control amplicon was labeled Cy3 (green). Both samples were cohybridized onto an ECIST microarray slide and processed as described (7).

Expression Microarray Analysis. Total RNA (100 µg) was prepared from control (vehicle treated) CP70 cells, or cells cultured with TSA and/or DAC. The RLCS method was used to generate full-length cDNAs. For quality control, the Rapid Amplification of cDNA Ends method was used to determine the integrity of 5'-ends of a few cDNA sequences (10). Cy5-labeled cDNAs from treated cells and Cy3-labeled cDNAs from untreated cells were cohybridized to the ECIST panel, and microarray images obtained were processed accordingly.

ChIP Microarray Analysis. The protocol used to identify immunoprecipitated E2F1 targets (2) was adapted for this study. To obtain a network of DNA-protein biopolymers, treated or untreated CP70 cells (2×10^7 cells/assay) were cross-linked using 1% formaldehyde. Cell nuclei were collected by microcentrifugation, and cross-linked chromatin fibers were isolated and fragmented to ~600-bp by sonication. Immunoprecipitation was carried out with 5 µg of antiacetylated histone H3 or H4 rabbit polyclonal antibody (Upstate) or no-antibody (negative control). DNA was additionally released by digesting the immunocomplex with proteinase K. Purified chromatin DNA (a total of ~1 µg) was recovered from 10–15 preparations for fluorescent labeling. Microarray hybridization, posthybridization washing, and slide scanning have been described previously by us (2).

Microarray Data Analysis. The Cy3 and Cy5 fluorescence intensities of hybridized ECIST spots were obtained for each experiment. Because Cy5 and Cy3 labeling efficiencies varied among samples, the Cy5: Cy3 ratio of each spot was normalized according to the global ratio in each microarray image. As described in our previous studies (7, 9, 10), the derived normalization factor

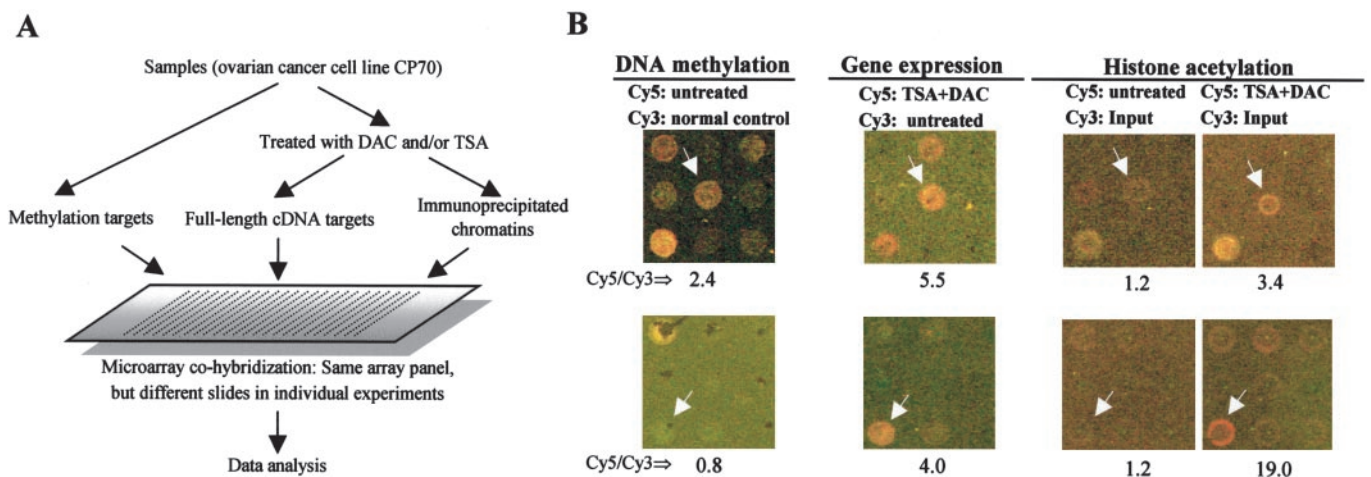


Fig. 1. A, schematic flowchart for parallel assessment of gene expression, DNA methylation, and histone acetylation in ovarian cancer cell line CP70. B, representative microarray images for the triple analysis. Cy5- and Cy3-labeled targets were prepared as described in the text and cohybridized to the ECIST microarray panel. The hybridization images were acquired, and signal intensities of ECIST spots (see examples marked by arrows) were calculated. The normalized Cy5: Cy3 ratios are shown at the bottom of each microarray panel image.

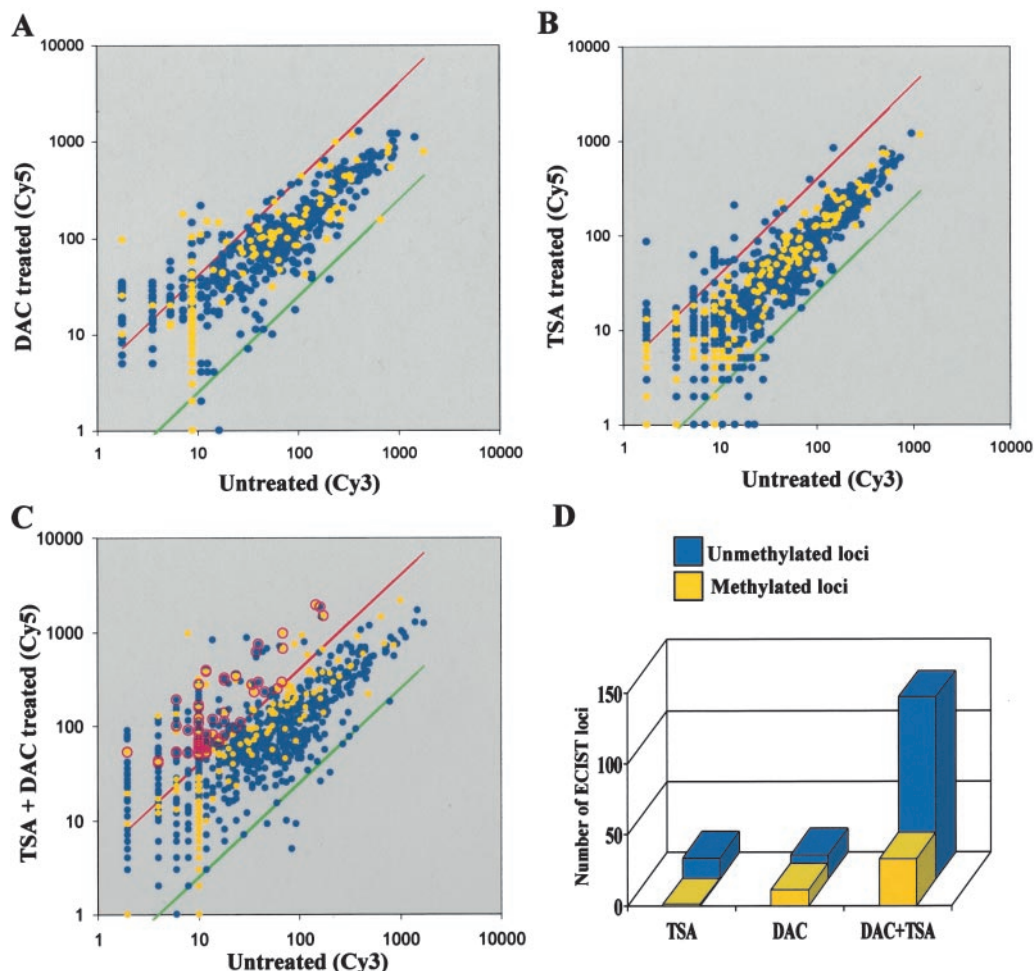


Fig. 2. Scatter plots (A–C) of the triple analysis in CP70 cells using the ECIST microarray panel. Microarray hybridization was conducted as described in the text. Cy5: Cy3 ratios of ≥ 4 (red line) or ≤ 0.25 (green line) were used to identify up- or down-regulated genes, respectively, in response to epigenetic treatments. Yellow and blue spots depict hypermethylated and unmethylated loci, respectively, in CP70 cells. Red circles indicate hyperacetylated ECIST loci identified by microarray analysis (see additional description in the text). D, total number of up-regulated ECIST loci in response to various epigenetic treatments.

was additionally verified based on 14 internal controls of which the adjusted ratios were expected to be 1. Microarray experiments were repeated twice. A self-hybridization study using two equal portions of a test DNA sample was conducted for quality control. These self-hybridizing spots usually had adjusted Cy5: Cy3 ratios approaching 1.

Nucleotide Sequencing. Plasmid DNA was prepared from ECISTs and sequenced using the DyeDeoxy Terminator reaction (Applied Biosystems) and the ABI PRISM 377 sequencer. The sequencing results were compared with GenBank for known sequence identities.

COBRA. Sodium bisulfite modification of genomic DNA, which converts unmethylated but not methylated cytosine to uracil, was performed using the CpG Genome modification kit (Intergen). COBRA was performed as described (13). Briefly, ~ 200 ng of treated DNA were used as the template for PCR with specific bisulfite primers (Table 1) for a given locus. 32 P-labeled PCR products were digested with *Bst*UI, separated on 8% polyacrylamide gels, and subjected to autoradiography using a PhosphorImager (Amersham-Pharmacia).

Semiquantitative RT- and ChIP-PCR. cDNA and chromatin DNA were prepared as described earlier. Diplex PCR (for both test and control targets) was performed using the AmpliTaq Gold polymerase (Perkin-Elmer). For RT-PCR, primer pairs were used to amplify a region (average 200-bp) from the 3'-end of a test gene, whereas for ChIP-PCR, primers were designed to amplify a fragment in the promoter or first exon region (average 200-bp) of the test gene (see Table 1 for primer information). After 20–25 cycles of amplification, radiolabeled PCR products were run on 5–8% polyacrylamide gels. A PhosphorImager was used to analyze the dried gels, and densitometric analysis of the observed bands was performed using ImageQuant (Molecular Dynamics).

The relative levels of gene expression or histone acetylation were normalized with the level of the control run in the same lane.

RESULTS

ECIST Microarray. Using RLCS, we screened a library of ~ 9000 CGIs (12) and recovered 1,507 ECIST-positive loci. To confirm whether these ECISTs were located at the 5'-ends of genes, nucleotide sequencing was performed on 250 of these loci. Sequencing data showed that: (a) 79% (198) contained sequences located in the promoter and first exon of known genes; (b) 16% (40) matched genomic sequences and may contain as yet uncharacterized expressed sequences; and (c) 5% (12) contained non-exon 1 expressed sequences. These results suggest that the ECIST loci identified here can be effectively used to assess epigenetic alterations in cancer cells.

Triple Microarray Screening. To assess gene expression, DNA methylation, and histone acetylation in parallel, CP70 cells were treated with a demethylating agent, DAC, and/or an inhibitor of HDACs, TSA, and then subjected to triple microarray procedures (Fig. 1A). Representative individual gene loci are marked by arrows in Fig. 1B. At a hypermethylated locus in untreated CP70 cells (Fig. 1B, top panels), DAC plus TSA treatments increased expression (normalized Cy5: Cy3 = 5.5) and histone hyperacetylation (3.4-fold relative to the control) of this gene. The combined treatment of DAC plus TSA

Table 2 List of methylation-dependent genes up-regulated by epigenetic treatments

Clone	Chromosome	Gene bank	Gene name	Description	Location
CpG17E7 ^a	11p15	NM.013250	<i>ZNF215</i>	Novel imprinted zinc finger protein 215	Promoter and 1st exon
CpG18A11 ^a	11q24	NM.001274	<i>CHEK1</i>	CHK1 checkpoint homologue (<i>S. pombe</i>)	Promoter and 1st exon
CpG18G8 ^a	19p12	NM.138330	<i>TIZ</i>	TRAF6-binding zinc finger protein	Promoter and 1st exon
CpG21B1 ^a	1q32	NM.015434	<i>DKFZP434B168</i>	DKFZP434B168 protein	Promoter and 1st exon
CpG27E8 ^a	19q13	AK023102	<i>FLJ13040</i>	Hypothetical protein FLJ13040	First exon
CpG42E10	18p11	ND ^b	Predicted gene	Twinscan gene predictions	First exon
CpG5B6 ^a	12q13	NM.000785	<i>CYP27B1</i>	Cytochrome P450, subfamily XXVIII	Promoter and 1st exon
CpG6B6 ^a	20p12	AL137678	<i>vyto</i>	SEL1L homologue	Promoter and 1st exon
CpG79F12 ^a	15q25	AL110434	EST	Function unknown	ND
MP2D2 ^a	2p14	ND	ND	Genscan gene predictions	ND
MP3F2	19p13	X06581	<i>ERCC-1</i>	DNA excision repair protein	Promoter
SC11E2 ^a	19p13	ND	ND	No gene identified in this region	ND
SC11H10	1q22	NM.032323	<i>MGC13102</i>	Hypothetical protein MGC13102	Exon 3
SC15E7 ^a	14q23	ND	Predicted gene	Genscan gene predictions	Promoter and 1st exon
SC15H6 ^a	6p21	NM.021058	<i>H2BFR</i>	H2B histone family, member R	First exon
SC18E9	19p13	X06581	<i>ERCC-1</i>	DNA excision repair protein	Promoter
SC18F11 ^a	12p13	ND	Predicted gene	Genscan gene predictions	ND
SC18C9	3q21	BI833804	<i>Seefor</i>	β -1,4 mannosyltransferase homologue	Exon 5
SC19F1 ^a	1q23	AB029012	<i>KIAA1089</i>	Hypothetical protein KIAA1089	Promoter and 1st exon
SC21G11 ^a	14q23	NM.021979	<i>HSPA2</i>	Heat shock 70kD protein 2	First exon
SC23B1	11q13	BI085096	<i>Reemay</i>	β -1,4 mannosyltransferase homologue	Exon 3
SC26B7 ^a	8p23	R18473	EST	Function unknown	ND
SC2A2	Xq13	ND	ND	No gene identified in this region	ND
SC33C8 ^a	2p23	NM.024322	<i>MGC11266</i>	Hypothetical protein MGC11266	Promoter and 1st exon
SC40C8 ^a	6p22	NM.003522	<i>H2BFG</i>	H2B histone family, member G	Promoter and 1st exon
SC4H4 ^a	6p21	NM.002121	<i>HLA-DPB1</i>	Major histocompatibility complex, class II, DP	Promoter and 1st exon
SC5A4 ^a	8q21	ND	<i>Sneyly</i>	Acemby gene predictions	First exon
SC5D3	15q22	NM.032857	<i>MRPL56</i>	β -Lactamase	Promoter and 1st exon
SC74D2	10q24	BG208726	<i>Kloymy</i>	Acemby gene predictions	Promoter and 1st exon
SC7B11 ^a	19q13	BE646494	<i>Sposee</i>	Acemby gene predictions	Promoter and 1st exon
SC87F10 ^a	1p36	NM.001412	<i>EIF1A</i>	Eukaryotic translation initiation factor 4C	Promoter and 1st exon
SC89F2	6q13	NM.018665	<i>HAGE</i>	DEAD-box protein	Promoter and 1st exon
SC89G2	6q13	NM.018665	<i>HAGE</i>	DEAD-box protein	Promoter and 1st exon
SC8A10	19q13	X06581	<i>ERCC-1</i>	DNA excision repair protein	Promoter

^a Hyperacetylated histones detected based on microarray analysis (see detail in the text).

^b Not determined.

also increased expression and histone hyperacetylation of a locus that was not hypermethylated in untreated CP70 cells (Fig. 1B, bottom panels).

The total number of ECISTs up-regulated ≥ 4 -fold by epigenetic treatments was determined. Treatment with DAC or TSA alone resulted in up-regulation of 29 (1.9% of 1507 loci) or 17 (1.1%) loci, respectively; however, a greater number of genes (150 or 10.4%; $P < 0.001$ versus either treatment alone) were up-regulated after the combined treatment (Fig. 2, A–C). The epigenetic treatments also resulted in down-regulation of a few ECIST loci (≤ 0.25 -fold), but this response was not the focus of our investigation. Histone hyperacetylation was measured in the combined treatment and scored when a locus showed a normalized Cy5: Cy3 ratio 2-fold greater in the treated cells than that of untreated cells (2). Using this cutoff, hyperacetylated loci were detected in 3.6% (55; red circles in Fig. 2C) of the 1507 ECISTs examined.

To identify hypermethylated ECISTs, a normalized Cy5: Cy3 ratio ≥ 1.5 relative to the control was used. This cutoff ratio was used by us to reliably identify hypermethylated CpG islands in various cancers (7, 9, 14). The genes up-regulated by the combined treatment of DAC plus TSA were additionally divided into two groups (Fig. 2D): hypermethylated (group 1, yellow spots; see Table 2) and no detectable methylation (group 2, blue spots; see Table 3). As shown in Fig. 2C, up-regulation of group 1 loci is more closely associated with histone hyperacetylation than that of group 2 loci (64%; 22 of 34 loci versus 28%; 33 of 116 loci).

Up-Regulation of Methylation-silenced Genes in Response to Epigenetic Treatments. Within group 1 genes, increased expression of only a few loci ($n = 11$) was observed after treatment with DAC alone; however, the combined treatment of DAC and TSA resulted in up-regulation of 34 loci (Fig. 2D). No significant change in expression of group 1 genes was seen in CP70 cells treated with TSA alone. To

confirm the microarray findings, three gene loci from Group 1 (*HSPA.2*, *CYP27B1*, and *EIF1A*) were additionally analyzed. Hypermethylation of the *HSPA.2* CpG island in CP70 cells was confirmed using COBRA (Fig. 3, row 1, left panel), and no expression of *HSPA.2* was detected in untreated CP70 cells using RT-PCR (Fig. 3, row 1, middle panel). However, *HSPA.2* expression was increased by DAC treatment, remained unchanged after treatment with TSA alone, and was markedly increased by the combined treatment of DAC and TSA (Fig. 3, row 1, middle panel). Furthermore, after treatment of CP70 cells with DAC plus TSA, histones H3 and H4 in the promoter region of *HSPA.2* were determined to be hyperacetylated using ChIP-PCR (Fig. 3, row 1, right panel). These results support previous reports (3, 4) that the concerted action of DNA demethylation and histone hyperacetylation resulted in synergistic re-expression of methylation-silenced genes.

In untreated CP70 cells, partial methylation of the *CYP27B1* CpG island was observed, and expression of *CYP27B1* was low; however, treatment of CP70 cells with DAC plus TSA resulted in histone hyperacetylation and increased expression of *CYP27B1* (Fig. 3, row 2). Contrariwise, despite the strong hyperacetylation observed at the *EIF1A* locus, expression of *EIF1A* remained largely unaffected by the epigenetic treatments. The *EIF1A* locus we identified, located on human chromosome 1 (15), was determined to be hypermethylated in CP70 cells by using COBRA. It has been reported that multiple copies of *EIF1A* exist at different chromosomal regions, e.g., chromosomes X and Y (16), and it seems reasonable to suggest that one or more of these loci remain unmethylated, and, thus, contribute to the basal expression of *EIF1A* detected by RT-PCR (Fig. 3, row 3).

Up-Regulation of Methylation-independent Genes in Response to Epigenetic Treatments. A total of 116 loci were up-regulated (≥ 4 -fold) by the epigenetic treatments (blue spots; see also Fig. 2D), but expression of these loci appeared to be unrelated to DNA meth-

Table 3 List of methylation-independent genes up-regulated by epigenetic treatments

Clone Name	Chromosome	Gene bank	Gene name	Description	Location
CpG10D4	4q34	ND ^a	ND	No gene identified in this region	ND
CpG11D4	14q31	ND	ND	No gene identified in this region	ND
CpG11G12	19q13	BI194899	ND	EST sequence	ND
CpG11H5 ^b	11q12	NM.022830	<i>FLJ22347</i>	Hypothetical protein FLJ22347	Promoter and 1st exon
CpG12E10 ^b	20p13	X17567	<i>snRNP B</i>	snRNP B protein	Promoter
CpG12F10 ^b	19q13	NM.013362	<i>ZNF225</i>	Zinc finger protein 225	Promoter and 1st exon
CpG13E10	16q24	AK056131.1	<i>MGC13198</i>	Hypothetical protein MGC13198	Promoter and 1st exon
CpG13F10	16q22	NM.014062	<i>ART-4</i>	ART-4 protein	Promoter and 1st exon
CpG14B4	6p22.2	NM.003543	<i>H4FH</i>	H4 histone family, member H	First exon
CpG14F10	8q11	X74794	<i>MCM4</i>	Maintenance deficient 4 homologue protein	Promoter and 1st exon
CpG15A3	18p11	ND	ND	No gene identified in this region	ND
CpG15B4	6p22	NM.003543	<i>H4FH</i>	H4 histone family, member H	First exon
CpG15F10 ^b	ND	ND	ND	Sequence not determined	ND
CpG18G1	10q11	ND	ND	No gene identified in this region	ND
CpG27E3 ^b	19q13	ND	ND	FGENESH Gene Predictions (C19001774)	Promoter and 1st exon
CpG28H8	ND	ND	ND	No matched sequence	ND
CpG32G1	1q21	NM.003528	<i>H2BFO</i>	H2B histone family, member Q	Promoter and 1st exon
CpG32H5	22q12	ND	ND	FGENESH Gene Predictions (C22000342)	Promoter and 1st exon
CpG42B6	ND	ND	ND	Sequence not determined	ND
CpG42B7	7q33	NM.033139	<i>CALD1</i>	Caldeson 1 transcript variant 4	Promoter and 1st exon
CpG64A4	19q13	NM.002287	<i>LAIR1</i>	Leukocyte-associated Ig-like receptor 1, isoform	Second intron
CpG64F10	21q21	AF142099.1	<i>ADAMTS5</i>	Disintegrin-like and metalloprotease	Promoter and 1st exon
CpG66A4	6p22	NM.003543	<i>H4FH</i>	H4 histone family, member H	First exon
CpG67D1	10q25	ND	ND	No gene identified in this region	ND
CpG6E6	17p11	BC020774	<i>GNF2</i>	Guanine nucleotide binding protein (G protein)	Promoter and 1st exon
CpG71A6	3q25	NM.022736	<i>FLJ14153</i>	Hypothetical protein FLJ14153	ND
CpG79B10 ^b	7p22	ND	ND	No gene identified in this region	ND
CpG79H5	5q13	ND	ND	No gene identified in this region	ND
CpG7A11	2q13	NM.019014	<i>Rpo1-2</i>	Similar to DNA-directed RNA polymerase I	Promoter and 1st exon
CpG7B6 ^b	2q37	ND	Predicted gene	Genscan gene predictions	ND
DL2C8	4q34	ND	ND	No gene identified in this region	ND
DL3D1 ^b	11q12	AK001301.1	<i>FLJ10439</i>	Hypothetical protein FLJ10439	Promoter
DL3D6	7q33	AK056225	<i>FLJ31663</i>	cDNA FLJ31663, similar to myotrophin	Promoter and 1st exon
DL3G3 ^b	19p13	NM.021235	<i>EPS15R</i>	Epidermal growth factor receptor substrate	Promoter and 1st exon
MP1A9 ^b	11q23	NM.000615	<i>NCAM1</i>	Neural cell adhesion molecule 1	Promoter and 1st exon
MP1G1 ^b	2q31	AB046824	<i>KIAA1604</i>	Hypothetic protein KIAA1604	First exon
MP2A6 ^b	ND	ND	ND	Sequence not determined	ND
MP2B9	6p21	NM.021064	<i>H2AFP</i>	H2A histone family, member P	Promoter and 1st exon
MP2G7 ^b	20q13	NM.007019	<i>UBE2C</i>	Ubiquitin carrier protein E2-C	Promoter and 1st exon
MP2G9	7q36	ND	ND	No gene identified in this region	ND
MP2H11 ^b	2p14	ND	Predicted gene	Twinscan gene predictions	ND
MP3B9	7p22	ND	ND	No gene identified in this region	ND
MP3E5 ^b	3q23	AB002330	<i>KIAA0332</i>	Human mRNA for KIAA0332 gene	Promoter and 1st exon
PY1B11 ^b	15q15	BQ417318	<i>Reepor</i>	Acemby gene predictions	First exon
PY1E1 ^b	1q21	NM.003548	<i>H4F2</i>	Histone H4 family 2	Promoter and 1st exon
PY1F6	20p12	AK055700.1	<i>C20orf30</i>	Chromosome 20 open reading frame 30	Promoter and 1st exon
SC10B6 ^b	3q26	NM.004991	<i>MDS1</i>	Myelodysplasia syndrome protein 1	Exon 2
SC10H3 ^b	ND ^a	ND	ND	Sequence not determined	ND
SC10H6	15q14	AB011132	<i>KIAA0560</i>	KIAA0560 protein	Promoter and 1st exon
SC10H9	4q34	ND	ND	No gene identified in this region	ND
SC11D12	ND	ND	ND	Sequence not determined	ND
SC12B7	7p15	NM.006547	<i>KOC1</i>	IGF-II mRNA-binding protein 3	Promoter and 1st exon
SC12E1	6p21	NM.003897	<i>IER3</i>	Immediate early response 3, isoform	Promoter and 1st exon
SC13C2 ^b	2p23	BC015430	Predicted gene	Similar to transcription factor AKNA	Promoter and 1st exon
SC13E11	5q22	NM.053000	<i>TIGA1</i>	TIGA1	Promoter and 1st exon
SC14F1	ND ^a	ND	ND	No gene identified in this region	ND
SC15A10 ^b	10q22	ND	Predicted gene	Twinscan gene predictions	ND
SC15A8 ^b	7p14	AA478133	<i>Beyku</i>	Acemby gene predictions	Promoter and 1st exon
SC15E3	Xq26	NM.006649	<i>SDCCAG16</i>	Serologically defined colon cancer antigen 16	Promoter and 1st exon
SC17A9	4q31	ND	ND	No gene identified in this region	ND
SC17C6	14q23	ND	ND	No gene identified in this region	ND
SC18B4	ND	ND	ND	Sequence not determined	ND
SC18E10	10p15	ND	ND	No gene identified in this region	ND
SC18E11	17p12	ND	Predicted gene	Genscan gene predictions	ND
SC18E12	ND	ND	ND	No gene identified in this region	ND
SC18H8	20q11	AF287265	<i>HCA90</i>	Hepatocellular carcinoma-associated antigen 90	Promoter and 1st exon
SC19D7	6q23	AA360824.1	<i>KIAA1798</i>	Hypothetical protein KIAA 1798	Promoter and 1st exon
SC19F4	ND	ND	ND	Sequence not determined	ND
SC22B8	1p31	AI435457.1	<i>FOXO3.e</i>	Forkhead box D3 transcript e	Promoter and 1st exon
SC22C6	19p13	ND	ND	No gene identified in this region	ND
SC28C11	1p13	NM.005645	<i>TAF2K</i>	TATA box binding protein (TBP)-associated	Promoter and 1st exon
SC29B12	1q21	NM.003557	<i>PIP5K1A</i>	Phosphatidylinositol-4-phosphate 5-kinase	Promoter and 1st exon
SC29G3	1q32	AL526221.1	<i>TatD-Dnase</i>	Acemby gene predictions	Promoter and 1st exon
SC2F9 ^b	4q34	ND	ND	No gene identified in this region	ND
SC37C8	ND	ND	ND	Sequence not determined	ND
SC37H3 ^b	19q13	AB028987.2	<i>C19orf7</i>	Chromosome 19 open reading frame 7	First intron
SC40H2	5q11	NM.021147	<i>UNG2</i>	Uracil-DNA glycosylase 2	Promoter and 1st exon
SC41C2	1q21	NM.003557	<i>PIP5K1A</i>	Phosphatidylinositol-4-phosphate 5-kinase	First exon
SC41D5	7p15	AI347402	EST	Function unknown	ND
SC4A11	19q13	NM.015953	<i>NOSIP</i>	eNOS interacting protein	Promoter and 1st exon
SC4B5	ND	ND	ND	Sequence not determined	ND
SC4G5 ^b	7q33	NM.145808	<i>LOC136319</i>	Granule cell differentiation protein	Promoter and 1st exon
SC4H11 ^b	11q24	ND	ND	No gene identified in this region	ND

Table 3 *Continued*

Clone Name	Chromosome	Gene bank	Gene name	Description	Location
SC5C5	7q11	BE258578	<i>Glojoy</i>	Acemby gene predictions	Promoter and 1st exon
SC62F2 ^b	5p14	ND	ND	No gene identified in this region	ND
SC66A7	6p22	NM.003537	<i>H3FL</i>	H3 histone family, member L	Promoter and 1st exon
SC69A9 ^b	5q11	NM.021147	<i>UNG2</i>	Uracil-DNA glycosylase 2	Promoter and 1st exon
SC71B6 ^b	20q11	AK027550.1	<i>ZNF341 e</i>	Zinc finger protein 341 transcript 2	First intron
SC71E3	1q25	NM.032678	<i>MGC3413</i>	Hypothetical protein MGC3413	First exon
SC71G10	19q13	AK024429	<i>RhoGEF.16</i>	Acemby gene predictions	Promoter
SC73E9	7p14	ND	Predicted gene	Genscan gene predictions	Exon 3
SC73G5 ^b	6p21	BC000893	<i>H2BFA</i>	H2B histone family, member A	Promoter and 1st exon
SC74C3	10p11	ND	ND	No gene identified in this region	ND
SC76D1	7p22	BI085096	<i>spoyka</i>	Acemby gene predictions	Promoter and 1st exon
SC76H9	19q13	AI571106.1	<i>DDX34</i>	DEAD/H (Asp-Glu-Ala-Asp/His) box polypeptide	Promoter and 1st exon
SC77F2	ND	ND	ND	Sequence not determined	ND
SC77F4 ^b	4q13	ND	Predicted gene	Genscan gene predictions	ND
SC77H8	8p22	NM.006094	<i>DLCL1</i>	Deleted in liver cancer 1	First exon
SC78C2	2q37	AI208033.1	<i>Dudor</i>	Acemby gene predictions	Exons 1 and 2
SC78D5	1p35	NM.001703	<i>BAI2</i>	Brain-specific angiogenesis inhibitor 2	Promoter
SC7E12 ^b	17p11	ND	ND	No gene identified in this region	ND
SC7H5 ^b	3p14	BC003364.1	<i>ARF4</i>	ADP-ribosylation factor 4.	Promoter and 1st exon
SC86B10	3p13	BI196363.1	<i>Glorfy</i>	Acemby gene predictions	Exon 2
SC86B2	4q34	ND	ND	No gene identified in this region	ND
SC86B9	6q13	NM.133645	<i>MTO1</i>	MTO1 protein isoform IV	Promoter and 1st exon
SC86G9	6q13	NM.012123	<i>CGI-02</i>	CGI-02 protein	Promoter and 1st exon
SC87G12	11q13	NM.053056	<i>CCND1</i>	Cyclin D1	Promoter and 1st exon
SC88C10	ND	ND	Predicted gene	Genscan gene predictions	ND
SC88C8	12p13	BG940697	EST	Function unknown	ND
SC88E12	12q13	NM.005371	<i>METTL1</i>	Methyltransferase-like protein 1, isoform a	Promoter and 1st exon
SC89A10	17q21	AK056941	<i>FLJ32379</i>	Polyprotein homologue	Promoter and 1st exon
SC89H7	12q23	AK001250.1	<i>FLJ10388</i>	Hypothetical protein FLJ10388, RNA polymerase	First intron
SC8D1	14q23	NM.002788	<i>PSMA3</i>	Proteasome (prosome, macropain) subunit, α	First exon
SC90B1	12p13	NM.000719	<i>CACNA1C</i>	Calcium channel, voltage-dependent, L type,	Exon 7
SC90B12	7p15	NM.006547	<i>KOC1</i>	IGF-II mRNA-binding protein 3	Promoter and 1st exon
SC90F10	9p23	ND	Predicted gene	Genscan gene predictions	ND

^a Not determined.

^b Hyperacetylated histones detected based on microarray analysis (see detail in the text).

ylation. From this group, 8 loci were additionally analyzed using COBRA, RT-PCR, and ChIP-PCR (Fig. 4, A and B). The loci were unmethylated in CP70 cells, and expression of these loci was low or absent in untreated CP70 cells. Increased expression of some of these loci was observed after treatment with DAC or TSA alone. The combined treatment induced expression of all 8 of the loci, but histone hyperacetylation was seen in only the promoter regions of *MDS1*, *SC13C2*, and *UNG2* (Fig. 4A). On the basis of the response of these 8 loci to the epigenetic treatments, we additionally subdivided the methylation-independent loci into two groups: group 2a, methylation-independent, histone acetylation-enhanced genes ($n = 33$) and group 2b, methylation- and histone acetylation-independent genes ($n = 83$).

DISCUSSION

To additionally define epigenetic modifications and order of epigenomic events at CpG islands on a global scale, we have developed a microarray system that combines gene expression, DNA methylation, and DNA-protein interaction analyses. To our knowledge, this represents the first report of a genomic approach that is capable of dissecting the complex hierarchy of transcriptional controls orchestrated by the epigenomic machinery. This integrated microarray system allows for both the identification of individual genes and a systematic analysis of the relationship among the epigenetic machinery, promoter targets, and downstream responses regulated by the epigenome.

It has been demonstrated that pharmacological reversal of promoter hypermethylation status results in global and specific changes in gene expression (3, 5); in addition, inhibiting DNA methylation has both primary (direct) and secondary (indirect) effects on gene expression (3, 17, 18). Using the triple analysis approach, we identified both primary and secondary responses, and additionally categorized those responses into three groups of genes based on their methylation status:

group 1, methylation-dependent, and groups 2a and b, methylation-independent. For group 1 genes, transcriptional silencing is dominated by methylation (Fig. 3). Reactivation of genes silenced by CpG methylation would presumably involve a series of steps, including removal of MBD proteins from demethylated DNA and/or transcriptional repressors that are recruited by MBD proteins (5). Epigenetic complexes have been shown to possess chromatin-remodeling activity and produce structures refractory to transcriptional activation (5). Disrupting these complexes would presumably diminish their activity and result in a more open, transcriptionally active chromatin configuration. A physical association between methylated DNAs and deacetylated histones has been shown recently (19), and our observation that synergistic reactivation of methylation-silenced genes (group 1) could only be achieved by the combined treatment is suggestive of a functional interaction between the epigenetic modifications. Whether this functional relationship is because of a direct or indirect interaction between the molecular targets remains to be elucidated.

The triple array analysis revealed an effect of the drug treatments on methylation-independent gene expression. Group 2a represents a class of distinct genes with unmethylated promoters of which the increased expression is produced by TSA alone or the combined treatment, but not by DAC alone. It is unclear how DAC and TSA act mechanistically on unmethylated promoters, but it was shown recently that DNA methyltransferase 1 (3), in the absence of DNA methylation, can directly suppress transcription through actions with HDACs (3, 19). Our observation that enhanced histone hyperacetylation of *MDS1* required both DAC and TSA supports a role for a methylation-independent effect of DNA methyltransferase 1 in ovarian cancer cells; furthermore, these observations indicate that HDAC activity may play a role in the epigenetic-associated control of group 2a gene expression. The majority of genes we identified in this triple array

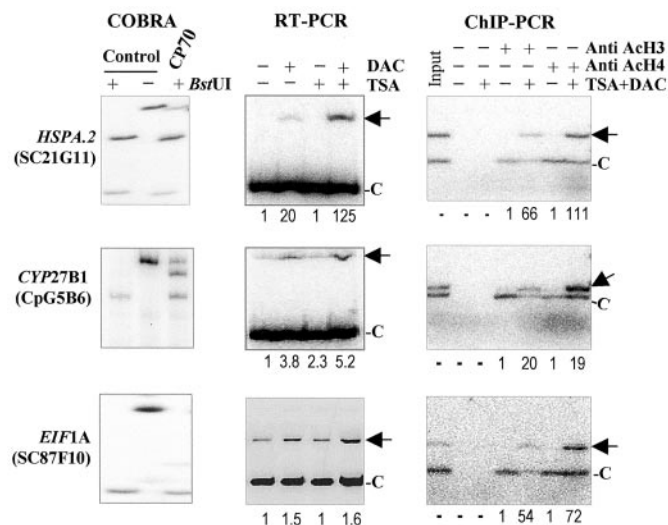


Fig. 3. Analysis of DNA methylation, gene expression, and histone acetylation in methylation-dependent ECIST loci. Methylation analysis: COBRA was used to determine the methylation status of ECIST loci in ovarian cancer cell line CP70 (gene names are shown at left). Genomic DNA (2 μ g) was bisulfite-treated and subjected to PCR using primers flanking the interrogating *Bst*UI site(s) in each ECIST locus. 32 P-labeled products were digested with *Bst*UI and separated on 8% polyacrylamide gels. As shown, the digested fragments reflect *Bst*UI methylation within a CpG island. Control DNA was methylated *in vitro* with the SSI methylase. +: *Bst*UI digestion; -: without *Bst*UI digestion. Expression analysis: total RNA (2 μ g) isolated from treated (+) or untreated (-) CP70 cells was used to generate cDNA for RT-PCR. Arrows indicate the positions of amplified fragments. The level of each ECIST expression was compared with that of β -actin (marked by C). Acetylation analysis: chromatin DNA was immunoprecipitated with antiacetylated histone 3 (*Anti Ach3*) or 4 (*Anti Ach4*) and subjected to PCR using primers located at the 5'-ends of a test gene. Arrows indicate the positions of amplified products. The level of histone acetylation for an ECIST locus was compared with that of a control locus (C), either *GTF2H4* or *FLJ31996*.

analysis belonged to group 2b, which showed enhanced expression independent of both DNA demethylation and histone acetylation. Up-regulation of these loci by DAC plus TSA treatments is most likely because of an event downstream of modulations in the epigenetic cascade. There are several possible, but not mutually exclusive, mechanisms that may account for this secondary effect, including increased post-transcriptional processing (RNA stability), reactivation of an upstream transcription factor, or regulation by target genes in an induced signal transduction pathway (20).

Induction of some of the genes in group 2 is likely to be associated with cellular responses to drug toxicity or stress, as shown recently by several groups using microarrays to examine gene expression profiles in DAC-treated human cancer cell lines (3, 17, 21). Furthermore, many of the stress-response genes induced by DAC show similar early and transient expression characteristics (21). For example, early induction of the apoptosis promoting factor *BIK* was observed after DAC treatment of a human lung cancer cell line, and *BIK* expression returned to control levels by 72 h after treatment with DAC (21). Interestingly, the *BIK* gene, which does not contain a CpG island, is also induced in a methylation-independent manner by TSA (3). In contrast, DAC treatment gradually induces expression of methylation-dependent genes and their downstream targets (17, 21), and expression of these genes has been shown to be prolonged or increased as demethylation progresses (17, 21). In this regard, our triple microarray system is well suited for distinguishing early stress-response genes from late genes induced by epigenetic treatments over time, and our future studies will investigate this and the effect of other modulators on epigenetic pathways.

The current study offers proof of principle for a triple microarray system capable of interrogating the complex hierarchy of epigenetic changes often seen in human cancer. This integrated approach is

useful for identifying novel therapeutic targets and more fully understanding the mechanisms underlying epigenetic gene silencing. The continued development of the triple microarray will be useful for assessing the specificity of emerging epigenetic therapies based on reactivating the expression of methylation-silenced genes in cancer and other diseases.

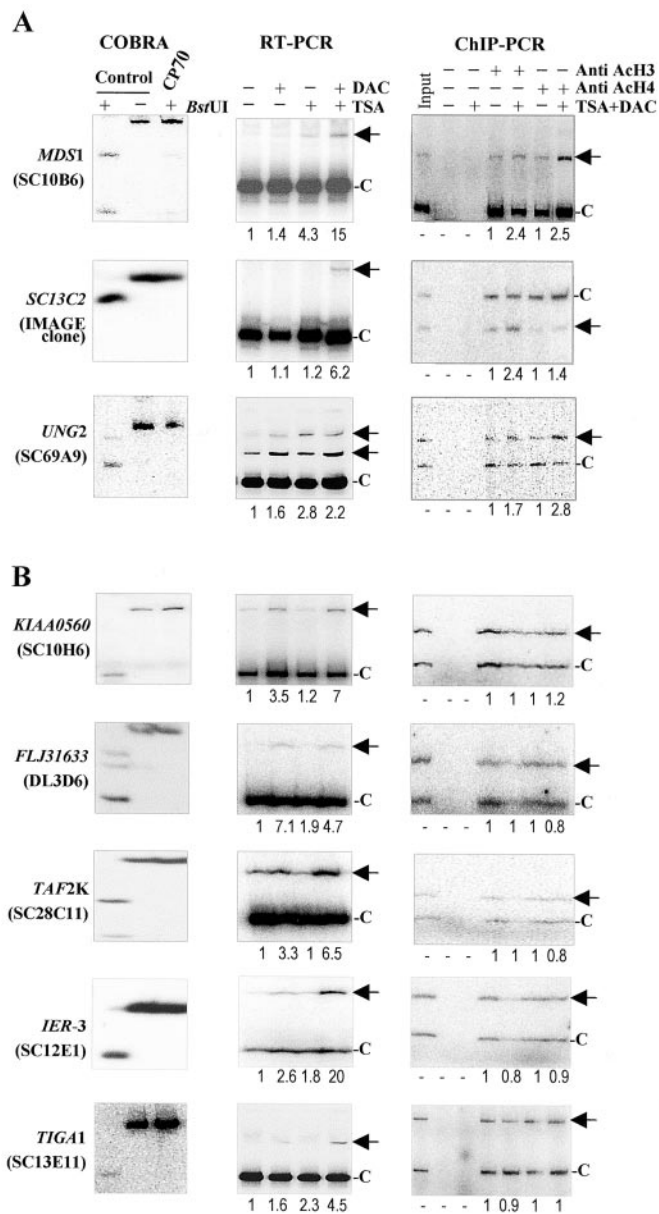


Fig. 4. Triple analysis of group 2a ECIST loci (A, methylation-independent and histone acetylation-enhanced) and group 2b loci (B, methylation- and histone acetylation-independent). See also "Results" section for nomenclature of group 2s. Methylation analysis: COBRA (combined bisulfite restriction analysis) was used to determine the methylation status of ECIST loci in ovarian cancer cell line CP70 (gene names are shown at left). Genomic DNA (2 μ g) was bisulfite-treated and subjected to PCR using primers flanking the interrogating *Bst*UI site(s) in each ECIST locus. 32 P-labeled products were digested with *Bst*UI and separated on 8% polyacrylamide gels. As shown, the digested fragments reflect *Bst*UI methylation within a CpG island. Control DNA was methylated *in vitro* with the SSI methylase. +: *Bst*UI digestion; -: without *Bst*UI digestion. Expression analysis: total RNA (2 μ g) isolated from treated (+) or untreated (-) CP70 cells was used to generate cDNA for RT-PCR. Arrows indicate the positions of amplified fragments. The level of each ECIST expression was compared with that of β -actin (marked by C). Acetylation analysis: CP70 cells were treated with DAC plus TSA (+) or untreated (-). Chromatin DNA was then immunoprecipitated with (+) or without (-) antiacetylated histone 3 (*Anti Ach3*) or 4 (*Anti Ach4*) and subjected to PCR using primers located at the 5'-ends of a test gene. Arrows indicate the positions of amplified products. The level of histone acetylation for an ECIST locus was compared with that of a control locus (C), either *GTF2H4* or *FLJ31996*.

ACKNOWLEDGMENTS

We thank Diane Peckham for assistance in the preparation of this manuscript.

REFERENCES

- Ren, B., Robert, F., Wyrick, J. J., Aparicio, O., Jennings, E. G., Simon, I., Zeitlinger, J., Schreiber, J., Hannett, N., Kanin, E., Volkert, T. L., Wilson, C. J., Bell, S. P., and Young, R. A. Genome-wide location and function of DNA binding proteins. *Science (Wash. DC)*, *290*: 2306–2309, 2000.
- Weinmann, A. S., Yan, P. S., Oberley, M. J., Huang, T. H-M., and Farnham, P. J. Isolating human transcription factor targets by coupling chromatin immunoprecipitation and CpG island microarray analysis. *Genes Dev.*, *16*: 235–244, 2002.
- Suzuki, H., Gabrielson, E., Chen, W., Anbazhagan, R., van Engeland, M., Weijnen, M. P., Herman, J. G., and Baylin, S. B. A genomic screen for genes upregulated by demethylation and histone deacetylase inhibition in human colorectal cancer. *Nat. Genet.*, *31*: 141–149, 2002.
- Cameron, E. E., Bachman, K. E., Myohanen, S., Herman, J. G., and Baylin, S. B. Synergy of demethylation and histone deacetylase inhibition in the re-expression of genes silenced in cancer. *Nat. Genet.*, *21*: 103–107, 1999.
- Jones, P. A., and Baylin, S. B. The fundamental role of epigenetic events in cancer. *Nat. Rev. Genet.*, *3*: 415–428, 2002.
- Ballestar, E., and Esteller, M. The impact of chromatin in human cancer: linking DNA methylation to gene silencing. *Carcinogenesis (Lond.)*, *23*: 1103–1109, 2002.
- Yan, P. S., Chen, C-M., Shi, H., Rahmatpanah, F., Wei, S. H., Caldwell, C. W., and Huang, T. H-M. Dissecting complex epigenetic alterations in breast cancer using CpG island microarrays. *Cancer Res.*, *61*: 8375–8380, 2001.
- Ahluwalia, A., Yan, P., Hurteau, J. A., Bigsby, R. M., Jung, S. H., Huang, T. H-M., and Nephew, K. P. DNA methylation and ovarian cancer. I. Analysis of CpG island hypermethylation in human ovarian cancer using differential methylation hybridization. *Gynecol. Oncol.*, *82*: 261–268, 2001.
- Wei, S. H., Chen, C. M., Strathdee, G., Harnsomburana, J., Shyu, C. R., Rahmatpanah, F., Shi, H., Ng, S. W., Yan, P. S., Nephew, K. P., Brown, R., and Huang, T. H-M. Methylation microarray analysis of late-stage ovarian carcinomas distinguishes progression-free survival in patients and identifies candidate epigenetic markers. *Clin. Cancer Res.*, *8*: 2246–2252, 2002.
- Shi, H., Yan, P. S., Chen, C. M., Rahmatpanah, F., Lofton-Day, C., Caldwell, C. W., and Huang, T. H-M. Expressed CpG island sequence tag microarray for dual screening of DNA hypermethylation and gene silencing in cancer cells. *Cancer Res.*, *62*: 3214–3220, 2002.
- Suzuki, Y., Yoshitomo-Nakagawa, K., Maruyama, K., Suyama, A., and Sugano, S. Construction and characterization of a full length-enriched and a 5'-end-enriched cDNA library. *Gene*, *200*: 149–156, 1997.
- Cross, S. H., Charlton, J. A., Nan, X., and Bird, A. P. Purification of CpG islands using a methylated DNA binding column. *Nat. Genet.*, *6*: 236–244, 1994.
- Xiong, A., and Laird, P. W. COBRA: a sensitive and quantitative DNA methylation assay. *Nucleic Acids Res.*, *25*: 2532–2534, 1997.
- Yan, P. S., Efferth, T., Chen, H. L., Lin, J., Rodel, F., Fuzesi, L., and Huang, T. H-M. Use of CpG island microarrays to identify colorectal tumors with a high degree of concurrent methylation. *Methods (Orlando)*, *27*: 162–169, 2002.
- Dever, T. E., Wei, C. L., Benkowski, L. A., Browning, K., Merrick, W. C., and Hershey, J. W. Determination of the amino acid sequence of rabbit, human, and wheat germ protein synthesis factor eIF-4C by cloning and chemical sequencing. *J. Biol. Chem.*, *269*: 3212–3218, 1994.
- Lahn, B. T., and Page, D. C. Functional coherence of the human Y chromosome. *Science (Wash. DC)*, *278*: 675–680, 1997.
- Liang, G., Gonzales, F. A., Jones, P. A., Orntoft, T. F., and Thykjaer, T. Analysis of gene induction in human fibroblasts and bladder cancer cells exposed to the methylation inhibitor 5-aza-2'-deoxycytidine. *Cancer Res.*, *62*: 961–966, 2002.
- Karpf, A. R., Peterson, P. W., Rawlins, J. T., Dalley, B. K., Yang, Q., Albertsen, H., and Jones, D. A. Inhibition of DNA methyltransferase stimulates the expression of signal transducer and activator of transcription 1, 2, and 3 genes in colon tumor cells. *Proc. Natl. Acad. Sci. USA*, *96*: 14007–14012, 1999.
- Robertson, K., Keymars, K., Gonzales, F., Velicescu, M., and Jones, P. Differential mRNA expression of the human DNA methyltransferases (DNMTs)1, 3a and 3b during the Go/G1 to S phase transition in normal and tumor cells. *Nucleic Acids Res.*, *28*: 2108–2113, 2000.
- Karpf, A. R., and Jones, D. A. Reactivating the expression of methylation silenced genes in human cancer. *Oncogene*, *21*: 5496–5503, 2002.
- Milutinovic, S., Zhuang, Q., Niveleau, A., and Szyf, M. Epigenomic stress response: Knock-down of DNA methyltransferase 1 triggers an intra S-phase arrest of DNA replication and induction of stress response genes. *J. Biol. Chem.*, *278*: (e-publication ahead of print), 2003.

Cancer Research

The Journal of Cancer Research (1916–1930) | The American Journal of Cancer (1931–1940)

Triple Analysis of the Cancer Epigenome: An Integrated Microarray System for Assessing Gene Expression, DNA Methylation, and Histone Acetylation

Huidong Shi, Susan H. Wei, Yu-Wei Leu, et al.

Cancer Res 2003;63:2164-2171.

Updated version Access the most recent version of this article at:
<http://cancerres.aacrjournals.org/content/63/9/2164>

Cited articles This article cites 20 articles, 9 of which you can access for free at:
<http://cancerres.aacrjournals.org/content/63/9/2164.full#ref-list-1>

Citing articles This article has been cited by 16 HighWire-hosted articles. Access the articles at:
<http://cancerres.aacrjournals.org/content/63/9/2164.full#related-urls>

E-mail alerts [Sign up to receive free email-alerts](#) related to this article or journal.

Reprints and Subscriptions To order reprints of this article or to subscribe to the journal, contact the AACR Publications Department at pubs@aacr.org.

Permissions To request permission to re-use all or part of this article, use this link
<http://cancerres.aacrjournals.org/content/63/9/2164>.
Click on "Request Permissions" which will take you to the Copyright Clearance Center's (CCC) Rightslink site.